Journal of Computer-Aided Molecular Design, 7 (1993) 45–60
ESCOM

J-CAMD 184

CoMFA validation of the superposition of six classes of compounds which block GABA receptors non-competitively

Julie A. Calder[a], John A. Wyatt[a,*], David A. Frenkel[a] and John E. Casida[b]

[a]*Department of Chemistry, Roussel Uclaf Environmental Health, Berkhamsted HP4 2DY, U.K.*
[b]*Pesticide Chemistry and Toxicology Laboratory, Department of Entomological Sciences, University of California, Berkeley, CA 94720, U.S.A.*

Received 24 April 1992
Accepted 22 August 1992

Key words: Steric alignment; Electrostatic alignment; Insecticidal activity; Picrotoxinin

SUMMARY

Thirty-six compounds, representing six different structural classes of insecticides which are known to act at the γ-aminobutyric acid receptor/chloride ionophore, have been superimposed by methods which maximise the commonality of steric and electrostatic fields. Maximal steric and electrostatic alignment was derived by pairwise comparisons of the different chemical classes with picrotoxinin. To test the validity of the combined superposition, a Comparative Molecular Field Analysis (CoMFA) was carried out within SYBYL, using recently published in vivo and in vitro binding data for insecticides. The resultant partial least-squares (PLS) analysis of sampled steric and electrostatic fields showed a significant statistical correlation with the published biological data. The predictive model obtained was shown to have a greater than 95% chance of significance.

INTRODUCTION

The γ-aminobutyric acid (GABA)-gated chloride channel is known to be the site of action of several classes of therapeutic agents and insecticides [1]. Within the ionophore complex, there are several distinct ligand binding regions, including benzodiazepine, barbiturate, avermectin and picrotoxinin binding sites. The physiological response to ligand-gated chloride ion modulation of the $GABA_A$-gated ionophore complex is highly dependent on the structural type of ligand involved. Clinically useful compounds which bind to the benzodiazapine receptor enhance the action of the inhibitory neurotransmitter GABA, conferring sedative, hypnotic, anxiolytic and anticonvulsant properties to the drugs. Anxiogenic benzodiazepines have also been described, for example, flumazenil [2] (ethyl-8-fluoro-5,6-dihydro-5-methyl-6-oxo-4H-imidazo[1,5]-[1,4]-benzodiazepine-3-carboxylate), which bind to the benzodiazepine recognition site with high affinity and

*To whom correspondence should be addressed.

prevent the agonist actions of other benzodiazepines. Most classes of compounds which interact with the picrotoxinin binding site non-competitively antagonise GABA-mediated chloride currents, conferring convulsant properties to the molecule. Relatively small structural modifications within the γ-butyrolactone series, drugs which are believed to act at the picrotoxinin receptor [3], can result in a reversal of the pharmacological profile, thereby conferring either sedative or convulsive activity. A recent publication by Deng et al. [4] highlights six structural classes of insecticides which appear to bind at or close to the picrotoxinin binding site. This work was facilitated by the use of a radioligand binding assay, developed with the tritiated probe 1-(4-ethynylphenyl)-4-*n*-[2,3-$^3H_2$]propyl-2,6,7-trioxabicyclo[2.2.2]octane ([^{3}H]EBOB). This class of compound has been the subject of a number of publications about its potent insecticidal activity [5,6]. The proposal that this diverse structural group of compounds binds to identical or overlapping ligand binding sites stimulated the current study, in which we superimposed the structures cited in Ref. [4]. For simplicity, the structure numbering system used in Ref. [4] was also adopted here. CoMFA [7] may provide a procedure to test the cogency of the resultant molecular alignment. The results of this CoMFA analysis should give an indication as to whether the differences in the steric and electrostatic fields of the aligned molecules can be correlated with their biological activities.

In this paper we report the results of a molecular graphics study, using the Steric and Electrostatic Alignment Program [8] (SEA4) for 36 of the compounds cited in Ref. [4]. The six chemical classes represented in this study are the bicycloctanes, dithianes, picrotoxin components, lindane and isomers, cyclodienes and the silatranes (Fig. 1). CoMFA analysis lends strong support to the multiple alignment proposed by the SEA4 program.

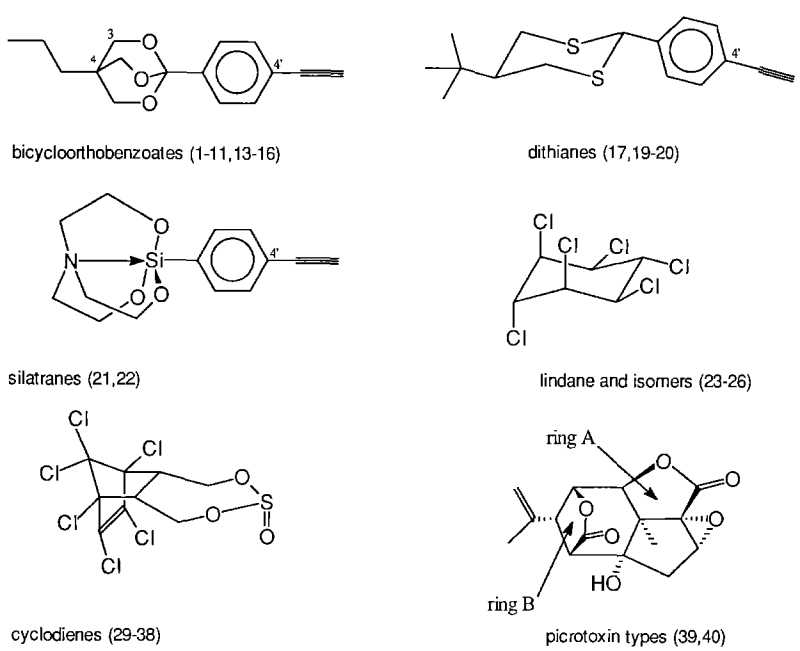

Fig. 1. Six structural classes of compounds believed to interact with the picrotoxin ligand binding site.

METHODOLOGY

Molecular modelling

The bicyclooctane and dithiane structures from Ref. [4] were modelled using the SYBYL molecular modelling software on a Silicon Graphics IRIS 4D25 workstation. These structures were fully optimised using MOPAC with the PM3 Hamiltonian [9]. Three-dimensional (3D) coordinates for the remaining compounds in the study, with the exception of α-endosulphan, were obtained from the Cambridge Crystallographic Database. It is noteworthy that the crystal structure for picrotoxinin was not significantly different from the fully optimised structure obtained by MOPAC/PM3 calculation. α-Endosulphan was modelled from the crystal structure of β-endosulphan by simple modification of the sulphur-containing ring, followed by full geometry optimisation using MOPAC/PM3. The PM3 method was used in preference to AM1 because it contained parameters for all of the atoms present, including sulphur. The MNDO method was not used because of the problem of over-estimation of the repulsions between atoms in the core repulsion function. It was felt that by adopting the technique of semi-empirical geometry optimisation, reasonable structures would be obtained for the molecules for which X-ray structures were not available.

Steric and electrostatic alignment

The molecules were sterically and electrostatically aligned using the QCPE program SEA4. In order for this procedure to be carried out, partial charges were required for each molecule. Gasteiger and Marsili charges were assigned using SYBYL. These charges were used in preference to the MOPAC-calculated charges, because of the presence of sulphur atoms in the dithiane and endosulphan molecules. It was considered that the use of an sp minimum basis set with sulphur, in particular, would not yield the best partial atomic charges for use in electrostatic comparisons, due to the inability to deal with the back-charge donation between 'p' and 'd' orbitals in the semi-empirical methods. Gasteiger and Marsili charges were calculated by a method which involved the equalisation of atomic electronegativities between bonded atoms. Eight π iterations were used to include the π orbitals in our calculations.

The molecules were aligned by using the SEA4 program, with picrotoxinin as the reference molecule in each case. The program fixes the position of the reference molecule and moves the second molecule to a random starting position with respect to the first molecule. Optimal electrostatic and steric complementarity between the molecules is achieved by the implementation of a simple two-component force-field algorithm. When the iterative fitting process is completed, molecule coordinates are recorded. This whole process is repeated a number of times (in our case 100), each time the relative starting geometry of the 'moving molecule' being set at random, and the best 20 fits based on the energy overlay term are stored. For this study, the electrostatic and steric contributions were set to have equal weighting. One member of each class of chloride channel agents (i.e., bicyclooctanes, dithianes, cyclodienes, silatranes and lindane isomers) was chosen to be sterically and electrostatically aligned with picrotoxinin. Picrotoxinin was selected for historical reasons (i.e., a well-characterised ligand binding site) rather than on the basis of affinity for the receptor, which is only moderate compared to that of the bicyclooctanes. The best overlay in each case was stored in a database as a proposed 'active-site orientation' of that molecule, along with the structure of picrotoxinin. Subsequently, all other members of each class

TABLE 1
STRUCTURES AND BIOLOGICAL DATA[a]

Structures[b]	In vitro binding data (IC_{50}, nM)	In vivo housefly data[c] (LD_{50}, μg/g)
1-Phenyltrioxabicyclooctanes		
(substituted at 4,4′ and 3 in one case)		
1 *n*-propyl, C ≡ CH (EBOB)	2.5	0.023
2 *t*-butyl,3-CN, C ≡ CH	3.8	0.024
3 *t*-butyl, C ≡ CH	3.9	0.011
4 *t*-butyl, C ≡ CMe	5.1	0.052
5 *c*-propyl, C ≡ CH	5.1	0.11
6 *c*-hexyl, Br	10	0.53
7 *c*-hexyl, Br	10.5	0.25
8 *t*-butyl, CN	11	0.23
9 *t*-butyl, Br	21	0.83
10 *s*-butyl, CN	33	1.0
11 Me_2 N, C ≡ CH	45	6.0
13 *t*-butyl, H	425	23.0
14 *t*-butyl, SMe	540	225
15 Me_2 N, Br	1000	130
16 *t*-butyl, *t*-butyl	> 10000	> 500
Dithianes		
(substitution at the 4′ position)		
17 C ≡ CH	8.1	0.11
19 H	155	12.5
20 Br	165	1.8
Silatranes		
(substitution at the 4′ position)		
21 C ≡ CH	245	3.4
22 Cl	> 10000	> 500
Lindane and isomers		
23 γ-lindane	11	0.93
24 α-lindane	2150	> 500
25 β-lindane	> 100000	> 500
26 δ-lindane	> 100000	> 500
Cyclodienes		
29 α-endosulfan	10	0.26
30 endrin	10	0.85
31 heptachlor-epoxide	17	0.55
32 dieldrin	31	0.82
33 β-endosulfan	35	1.55
34 α-chlordane	46	1.83
35 heptachlor	70	1.58
36 isodrin	109	1.7
37 aldrin	310	2.6
38 γ-chlordane	325	14.5
Picrotoxin components		
39 picrotoxinin	225	500
40 picrotin	6600	> 500

[a] The biological data and numbering system are reproduced from Ref. [4].
[b] See Fig. [1] for structural type.
[c] Oxidative detoxification was minimised by pretreatment with piperonyl butoxide to detect intrinsic potency better.

were RMS-fitted to the 'active-site orientation' of their aligned analogue. The new orientations of all molecules were stored in the database as 'active-site orientations'.

CoMFA analysis

A CoMFA was carried out on the aligned molecules, within the QSAR module of SYBYL, running on a Silicon Graphics 4D320 computer. CoMFA examines differences in target properties which are related to changes in the shape of the non-covalent (steric and electrostatic) fields surrounding the tested molecules. Details of the shape of each field are put into a QSAR table by sampling their magnitudes at regular intervals throughout a specified region of space. The alignment of the molecules is of crucial importance. CoMFA attempts to establish a relationship between the dependant variable or variables (usually biological activity) and the sampled steric and electrostatic fields within a defined region of Cartesian space at a user-defined grid resolution. Poorly aligned molecules would place random field values at the grid points, leading to poor cross validated R^2 values from the PLS analysis.

The quantitative structure–activity relationship (QSAR) is generated by carrying out a partial least-squares analysis of the CoMFA QSAR table, and the final results are examined by using graphics techniques.

The region over which the CoMFA fields (steric and electrostatic) were examined was calculated by noting the maximum and minimum x,y and z coordinates of all the aligned molecules. A region or 'box' was calculated whose x,y and z boundaries exceeded the maximum and minimum coordinates of every molecule in the database, by 4 Å in each direction. The target properties used in the PLS analysis were the in vivo or the in vitro data cited in Ref. [4]. The in vivo data, which are listed in Table 1, show toxicity to houseflies, measured as topical LD_{50} values at 24 h in the presence of piperonyl butoxide to inhibit oxidative detoxification, thus enabling a better approximation of intrinsic potency. The in vitro data, also listed in Table 1, were obtained by measurement of the inhibition of specific binding of [^{3}H]EBOB to housefly head membranes (presumably brain receptors) (IC_{50}). A discussion about the correlation between the in vivo and in vitro data can be found in Ref. [4]. Prior to analysis, the biological activity was transformed in the usual manner to the inverse logarithm.

Preliminary analyses were carried out using a crossvalidation technique [10]. This technique allows selection of the model which is most likely to have predictive value, i.e., it is used to establish the optimum number of components which best distinguish signal from noise. The initial preliminary analyses were carried out with eight components and ten crossvalidation runs. The effect of changing the grid resolution was examined, but the optimum used in this study, as discussed later, was 0.75 Å. It was also necessary to modify the value of 'minimum sigma' during crossvalidated runs. The inclusion of a minimum sigma value in the PLS analysis speeds PLS computation by omitting columns whose variance is less than a user-defined value. We found that a value of 1.3 for minimum sigma gave a good balance between computational speed and the quality of the data for our studies.

Since crossvalidation proceeds by omitting a specified number of random rows of input data, re-deriving the model and predicting the target properties of the omitted rows, the crossvalidated R^2 values often vary between runs. For this reason, the preliminary analyses were repeated with varying numbers of crossvalidation runs, to establish the best number of components to use. In the case of both the in vivo and in vitro data, the optimum number of components was found to

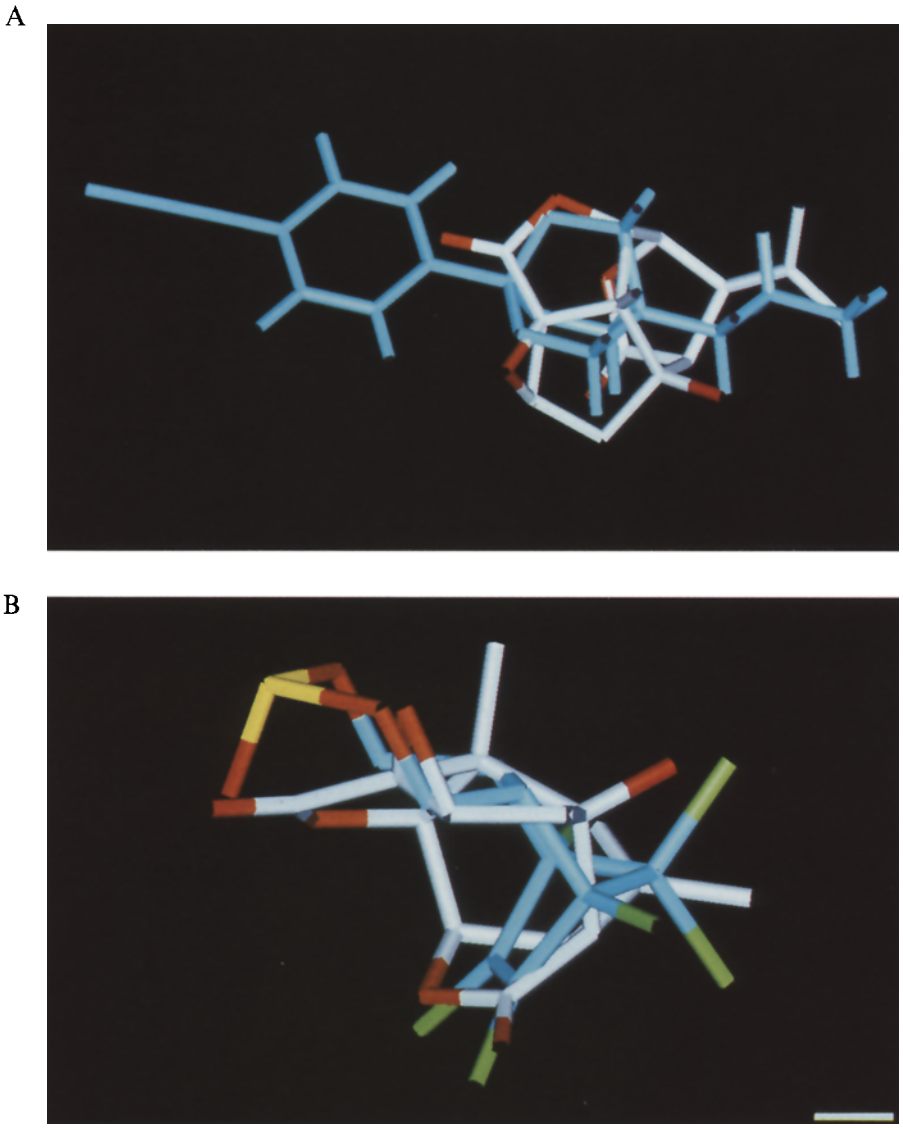

Fig. 2. (A) SEA4 overlay of picrotoxinin with a bicyclooctane; (B) SEA4 overlay of picrotoxinin and α-endosulfan.

be five. After the optimum number of components had been determined, the minimum sigma value was reset to zero and the final PLS analysis, without crossvalidation, was carried out for each set of data, and the final R^2 value was recorded in each case.

The results of the CoMFA QSAR were plotted by contouring the electrostatic and steric terms separately. In this study, the product of the standard deviation and the coefficient for each CoMFA column was used to plot the results. We felt that this method was more likely to show where changes in the steric and electrostatic fields were most highly associated with differences in activity.

C

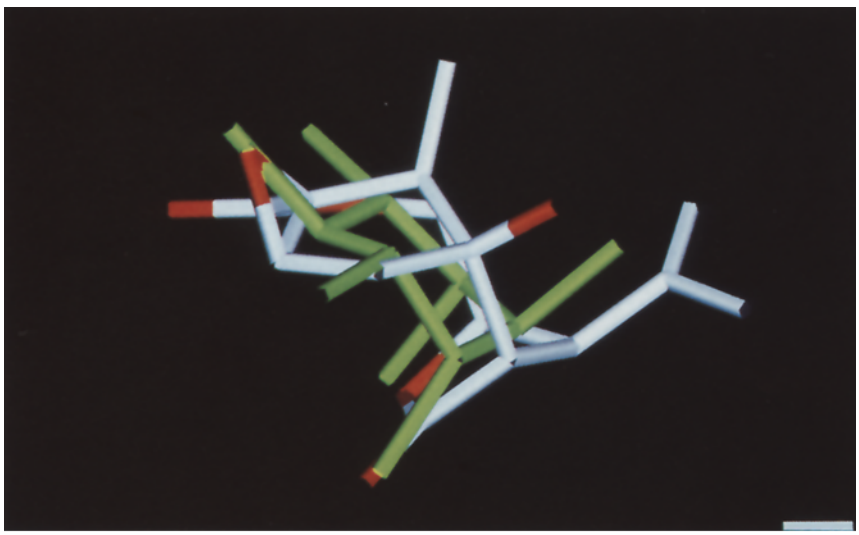

D

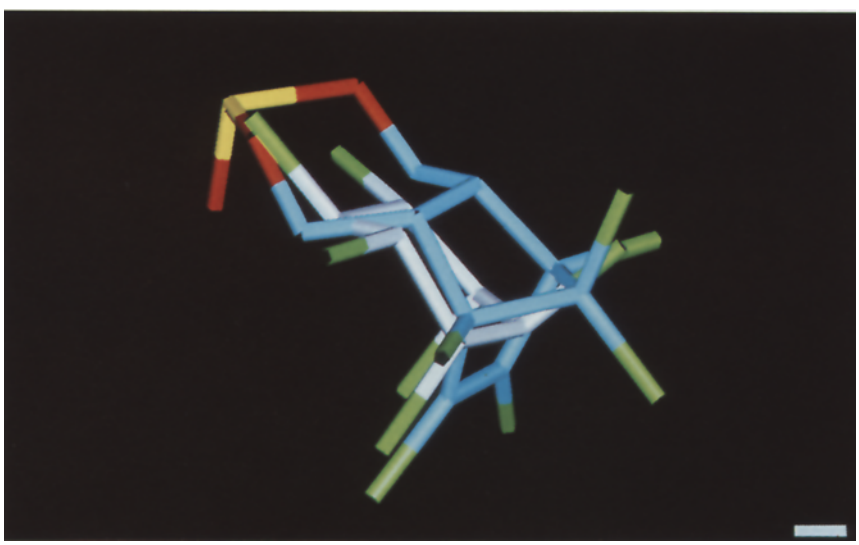

Fig. 2. (C) SEA4 overlay of picrotoxinin and γ-lindane; (D) SEA4 overlay of α-endosulfan and γ-lindane.

RESULTS AND DISCUSSION

Steric and electrostatic overlays

The steric and electrostatic overlays of picrotoxinin with the bicyclooctanes, the cyclodienes and the lindanes are illustrated in Figs. 2A–C respectively. By extrapolation, Fig. 2D shows the superposition of one of the HCH isomers with the cyclodienes. In the bicyclooactane overlay (Fig. 2A), an important region of overlap is the epoxy oxygen atom and the lactone ring oxygen atom (ring A in Fig. 1) of picrotoxinin, which overlay with two of the bicyclooctane cage oxygen

atoms. The isopropenyl group of picrotoxinin also overlays with the *n*-propyl or *t*-butyl group of the bicyclooctanes. The phenyl substituent at the 1-position of the bicyclooctane cage does not superimpose with any part of the picrotoxinin molecule, hence it is thought that the binding sites of the two structural classes must overlap. The dithianes and silatranes appear to have binding sites which completely superimpose with the bicyclooctane site, and hence also overlap with the picrotoxinin binding site. In the case of cyclodiene (Fig. 2B), an important region of overlap is with two of the oxygen atoms of the cyclic sulphite moiety of α-endosulphan, which are coincident with the epoxy oxygen atom and the lactone carbonyl oxygen atom of ring A of picrotoxinin. The second lactone ring of picrotoxinin (ring B in Fig. 1) also overlays with the chlorine-substituted double bond of α-endosulphan. In the γ-lindane overlay (Fig. 2C), the fit is less convincing, although there is good overlap of one of the equatorial chlorine atoms with the epoxy oxygen atom of picrotoxinin. Two of the axial chlorine atoms occupy a similar region of space as the lactone ring B of picrotoxinin, closely mimicking the situation with α-endosulphan. It is interesting to note that the less active isomers of lindane have either no or only one chlorine atom in this position. The overlay obtained using the SEA4 program was very similar to that suggested by Ozoe and Matsumura [11] in that the two rings at the 1-, 2- and 6-positions of picrotoxinin appear to correspond to the three equatorial chlorine atoms of lindane. However, in our calculations, the overlay of the central axial chlorine of γ-lindane and the isopropenyl group of picrotoxinin is not as close as suggested in Ref. [11]. The binding sites of the cyclodienes and the lindane isomers appeared to superimpose completely on the binding site of picrotoxinin.

CoMFA results

The results of the crossvalidated and final analyses on the in vivo data are shown in Tables 2 and 3. Table 2 shows the change in predictive R^2 during one in vivo crossvalidated analysis, as the number of components extracted and regressed increased from one to seven. The crossvalidation analysis resulted in five significant components being extracted for the in vivo data. These were regressed to give an in vivo QSAR model with a predictive R^2 of 0.43. If the biological data and the CoMFA parameters were truly unrelated, this QSAR would only have a 1.4% probability of occurring by chance. Replacement of the target data with a new set of random data, with the same mean and standard deviation as the original, resulted in equivalent R^2 values of −0.449, −0.651, −1.041, −1.437 and −1.362 for one to five components, respectively. Hence, we felt that our model, with a predictive R^2 value of +0.43, would be statistically likely to produce useful predictions. We should mention a cautionary note at this point; that a five-component non-crossvalidated regression model based on the random data gave a non-crossvalidated R^2 value of 0.7, which indicates how much noise can be extracted with the first five components. It is for this reason that we were careful to use the crossvalidated or 'predictive' R^2 values to evaluate the validity of our QSAR models.

The graph of predicted vs. actual activity for the crossvalidated in vivo analysis (Fig. 3) shows that the worst outliers (i.e., the compounds with the largest residual values) were γ-lindane, α-lindane, bicyclooctane-16, α-endosulphan and β-lindane. It is interesting to note that two of the five worst outliers, namely bicyclooctane-16 and β-lindane, have insecticidal LD_{50} values > 500 μg/g, which we arbitrarily set to 1000 μg/g for the purposes of the analysis. In every case where the endpoint for the biological data was unclear, and the IC_{50} or LD_{50} was quoted as greater than a particular value, we doubled that value for the purposes of the analysis. Since three of the five

worst outliers were also lindane isomers, it is possible that our chosen 'active-site orientation' for this class of compounds was not the optimum orientation. However, for consistency, we decided to continue using the best SEA4 overlay of the lindane isomers with picrotoxinin. The final analysis with five components was used to plot the CoMFA fields for the in vivo analysis.

The results of the crossvalidated and final analyses of the in vitro data are shown in Tables 4 and 5. Table 4 shows the change in predictive R^2 during one in vitro crossvalidated analysis, as the number of components extracted and regressed increased from one to seven. The in vitro crossvalidation analysis also resulted in five significant components being extracted. These were regressed to give an in vitro QSAR model with a predictive R^2 value of 0.44. Although this R^2 value is virtually the same as that obtained for the in vivo data, as were the CoMFA fields resulting from the non-crossvalidated final analysis, inspection of the predicted vs. observed in vitro activities shown in Fig. 4 would suggest that a significant proportion of this predictive R^2 value is due to the high leverage exerted by the two least-active lindane isomers. It will be noted that with the exception of these two compounds, the range of in vitro activity ($\times 10^{3.5}$) was

TABLE 2
DETAILS OF THE CROSSVALIDATED CoMFA ANALYSIS USING IN VIVO DATA

Minimum Sigma	1.3
Components	7
Crossvalidation runs	5

Component	R^2 value	Component	R^2 value
1	0.046	5	0.433
2	0.145	6	0.425
3	0.197	7	0.404
4	0.328		

Molecule	Residual value	Molecule	Residual value	Molecule	Residual value
Bicyclooctane-1	0.793	Bicyclooctane-14	−1.375	α-Endosulfan	2.573
Bicyclooctane-2	0.388	Bicyclooctane-15	−0.266	Endrin	1.122
Bicyclooctane-3	1.331	Bicyclooctane-16[a]	−2.630	Heptachlor epoxide	0.563
Bicyclooctane-4	0.491	Dithiane-17	0.269	Dieldrin	0.607
Bicyclooctane-5	0.496	Dithiane-19	−0.322	β-Endosulfan	−0.100
Bicyclooctane-6	−0.489	Dithiane-20	−0.054	α-Chlordane	0.664
Bicyclooctane-7	0.613	Silatrane 4′-alkynyl	1.093	Heptachlor	−0.207
Bicyclooctane-8	0.439	Silatrane 4′-chloro[a]	−0.777	Isodrin	−0.160
Bicyclooctane-9	0.881	γ-Lindane	3.269	Aldrin	−0.138
Bicyclooctane-10	−0.445	α-Lindane[a]	−2.735	γ-Chlordane	−0.872
Bicyclooctane-11	−0.442	β-Lindane[a]	1.490	Picrotoxinin	−0.168
Bicyclooctane-13	−0.682	δ-Lindane[a]	0.163	Picrotin[a]	−0.714

[a] When the endpoint of the biological data was unclear, and when quoted LD_{50} values exceeded a given value, we doubled the value for the analyses.

TABLE 3
DETAILS OF THE FINAL CoMFA ANALYSIS USING IN VIVO DATA

Minimum Sigma	0
Components	5
Crossvalidation runs	0
R^2 value	0.892
F value	46.374

significantly less than that for the in vivo data ($\times 10^{5.0}$). The worst outliers in the predicted vs. actual activity graph shown in Fig. 4 were bicyclooctane-16, γ-lindane, α-lindane and α-endosulphan, as with the in vivo analysis, and also picrotin. Three of these compounds were inactive (bicyclooctane-16) or had very low activity (α-lindane and picrotin). Of the others, α-endosulfan may be bio-oxidised to the corresponding sulphate, which is also active. Although lindane is a competitive inhibitor of [^{3}H]EBOB binding [4], it appears from unpublished studies from the Berkeley laboratory that it is a more selective inhibitor than the other types of compounds in the studies with houseflies vs other species. An alternative explanation for the poor predicted lindane values could be that the alignment of the molecules was incorrect. It is known that lindane and its isomers are somewhat unusual in that they show significant species specificity with respect to toxicological activity, which may suggest that the ligand–receptor interaction is somewhat different to that of the other molecules acting at this site. The final analysis, using five components, was used to plot the CoMFA fields for the in vitro analysis.

After the full PLS analyses had been completed with the in vivo and in vitro data, the steric and electrostatic fields were extracted from the QSAR table and plotted, using contour plots. Since the influence of each CoMFA coefficient is also dependent on the overall variance of the CoMFA values at each particular grid point, the 3D fields that were plotted are the products of the

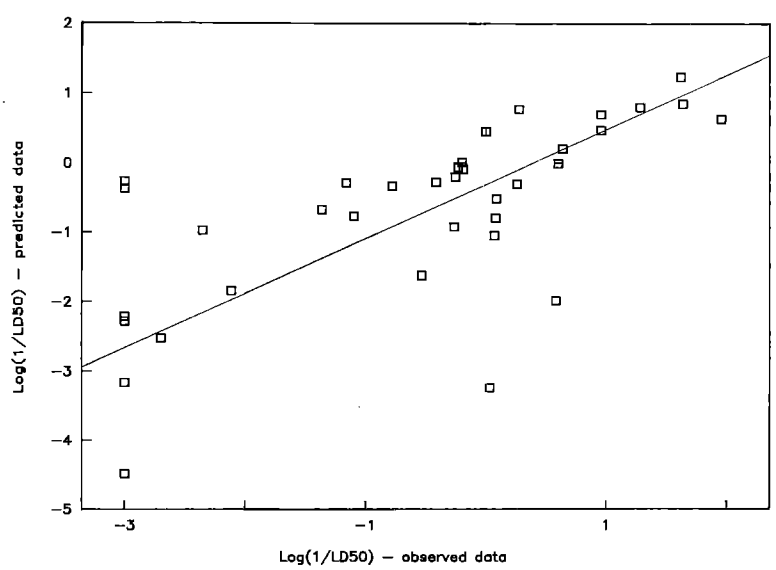

Fig. 3. Predicted vs. actual activities for crossvalidated analysis with in vivo data.

TABLE 4
DETAILS OF THE CROSSVALIDATED CoMFA ANALYSIS USING IN VITRO DATA

Minimum Sigma	1.3
Components	7
Crossvalidation runs	5

Component	R^2 value	Component	R^2 value
1	0.084	5	0.440
2	0.186	6	0.429
3	0.193	7	0.396
4	0.324		

Molecule	Residual value	Molecule	Residual value	Molecule	Residual value
Bicyclooctane-1	0.914	Bicyclooctane-14	−0.201	α-Endosulfan	1.854
Bicyclooctane-2	−0.149	Bicyclooctane-15	−0.804	Endrin	1.445
Bicyclooctane-3	0.475	Bicyclooctane-16[a]	−2.542	Heptachlor epoxide	0.534
Bicyclooctane-4	0.446	Dithiane-17	0.250	Dieldrin	0.413
Bicyclooctane-5	0.557	Dithiane-19	0.337	β-Endosulfan	−0.155
Bicyclooctane-6	0.001	Dithiane-20	−0.575	α-Chlordane	0.944
Bicyclooctane-7	0.353	Silatrane 4′-alkynyl	0.881	Heptachlor	−0.168
Bicyclooctane-8	0.300	Silatrane 4′-chloro[a]	−0.971	Isodrin	−0.309
Bicyclooctane-9	1.095	γ-Lindane	2.429	Aldrin	−0.514
Bicyclooctane-10	−0.596	α-Lindane[a]	−1.903	γ-Chlordane	−0.721
Bicyclooctane-11	0.427	β-Lindane[a]	0.884	Picrotoxinin	0.980
Bicyclooctane-13	−0.768	δ-Lindane[a]	−0.114	Picrotin	−1.792

[a] When the endpoint of the bistological data was unclear, and when quoted LD_{50} values exceeded a given value, we doubled the value for the analyses.

standard deviation and the coefficient for each column (STDDEV × COEFF). Figures 5A, 5B, 6A, and 6B show the steric and electrostatic CoMFA fields for the in vivo and in vitro data, respectively. The levels contoured correspond to grid points containing the 15% most negative values of STDDEV × COEFF (blue) and the 15% most positive corresponding values (red). Contoured areas containing open polyhedra are a result of missing grid point values, due to the grid point being within a common excluded molecular volume or because the variance at that point was less than the minimum sigma value specified for that particular analysis.

Interpretation of the fields

In theory, the CoMFA fields can be used to mofidy a molecular structure to obtain a better target property, by moving steric bulk closer to the regions of negative coefficients (red) and further from the regions of positive coefficients (blue). Similarly, in the electrostatic graphs, positive charge can be moved closer to the regions of positive coefficients (blue) and negative charge can be moved closer to the regions of negative coefficients (red). One problem of over-interpretation of the fields is that the molecules were overlaid rigidly, and no allowance was made

TABLE 5
DETAILS OF FINAL CoMFA ANALYSIS USING IN VITRO DATA

Minimum Sigma	0
Components	5
Crossvalidation runs	0
R^2 valve	0.917
F value	61.662

for the possible rotation of flexible groups in the molecules, e.g., the thiomethyl group of bicyclooctane-14, the phenyl rings of all the bicyclooctanes and dithianes, and the isopropenyl group of picrotoxinin. It is possible to include several different conformations for each molecule in the CoMFA analysis to account for rotational flexibility, but in this particular study we decided to use only X-ray structures or PM3-optimised geometries for simplicity. It is noticeable, that the CoMFA steric fields for the in vivo and in vitro data (Figs. 5A and 6A) were very similar. The CoMFA electrostatic fields for the in vivo and in vitro data (Figs. 5B and 6B) also showed remarkable consistency. Looking at the CoMFA fields more closely, it is immediately apparent that the presence of a 4-ethynyl substituent on the phenyl ring of the bicyclooctanes increases their insecticidal activity by contributing a strong electronegative potential in this region. The CoMFA fields show that steric bulk and a strong positive electrostatic potential are favourable in the region above the triple bond of the bicyclooctanes, as shown by the red contours in this region (Figs. 5 and 6). This can be illustrated by bicyclooctanes 3 and 4, which are both highly active, as they have a 4-ethynyl and a 4-propynyl phenyl substituent, respectively, and hence a positively charged hydrogen or methyl substituent in this region. Greater steric bulk in the region around the 4-ethynyl substituent itself is obviously detrimental to activity, as shown by the large blue area to the right of the triple bond in Figs. 5A and 6A. This result will have been caused by

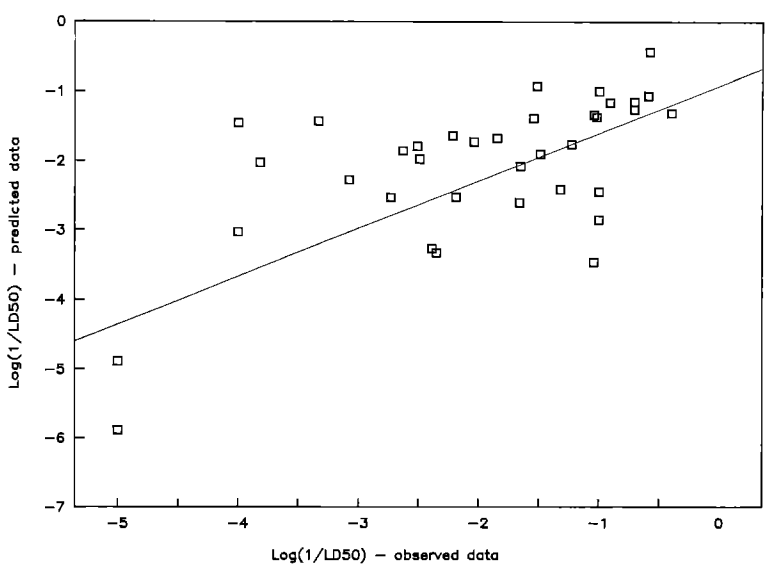

Fig. 4. Predicted vs. actual activities for crossvalidated analysis with in vitro data.

the lateral bulk of the 4'-*tert*-butyl group of bicyclooctane-16, and the 4'-thiomethyl group of bicyclooctane-14, both of which occupy this region of space and apparently reduce the insecticidal activity of these particular molecules.

In the region of the 4-substituent of the bicyclooctane molecules, the electrostatic CoMFA fields (Figs. 5B and 6B) indicate that a weakly positive electrostatic potential would be beneficial to activity. This result may have been caused by the presence of the 4-alkyl substituents of the most active class of insecticides, the bicyclooctanes. The electrostatic fields of these molecules are dominated by their numerous hydrogen atoms, which have small positive partial charges and which occupy this region of space. Other classes of insecticide, such as the cyclodienes, have predominantly negative electrostatic fields in this region, due to the presence of their chlorine substituents. However, as the cyclodienes are not as active as the bicyclooctanes, the overall result of the CoMFA analysis suggests that higher activity is associated with a more positive electrostatic potential in this region of space. In some respects, this may be a misleading result, as it is certainly possible that the higher activity of the bicyclooctanes could be because they occupy an additional binding area of the target site, rather than because they have a weak positively charged substituent at the 4-position. The steric CoMFA field around the 4-substituent of the bicyclooctanes indicates that an *n*-propyl group is favourable for activity, whereas a *tert*-butyl group is optimal in bulk.

The central section of the electrostatic CoMFA fields is the region where all of the insecticidal molecules overlap, hence this region is highly complex and difficult to interpret. It is in the central region that the electrostatic fields of the molecules are most alike and hence the effect of minor differences in their fields may be misleading when related to their activities. Differences in activity may be wrongly attributed to small changes in the electrostatic fields in this region, when in fact they are more likely to be due to the greater differences in the electrostatic fields of other parts of the molecules. We could find no clear trends in this central region. However, the steric CoMFA fields in this region revealed that steric bulk in the area of space containing the double bond of the cyclodienes and the γ-lactone ring of picrotoxinin would considerably enhance activity. There was also a clear indication that steric bulk in the region of the axial chlorine atom of γ-lindane would also enhance activity.

Grid resolution

At the start of this study, we accepted a default grid spacing of 2 Å, as suggested in the SYBYL manual. Crossvalidated PLS analysis of the resulting CoMFA matrix again extracted five significant components. However, when the corresponding non-crossvalidated run was produced and the resulting QSAR inspected as two 3D contour plots, it was noted that the electrostatic field (STDDEV × COEFF) in the region of the 4-substituent on the phenyl ring of the bicyclooctane, dithiane or silatrane was markedly asymmetric. As the only 4-substituents in this study were axially symmetric halogens or ethynyls, it was felt that this asymmetry must arise as a consequence of the high value of the grid spacing relative to the bond lengths/van der Waals distances involved. Thus as represented in Fig. 7, where the distance between grid points x_1 and x_2 is 2 Å, and typically C ≡ C is 1.2 Å, one may expect the electrostatic potentials or other CoMFA fields to be different at x_1 and x_2.

Indeed, when the grid spacing was reduced to 0.75°A and the analysis repeated, this field asymmetry in the region of the 4-substituent was removed entirely. It should be stressed that this

A

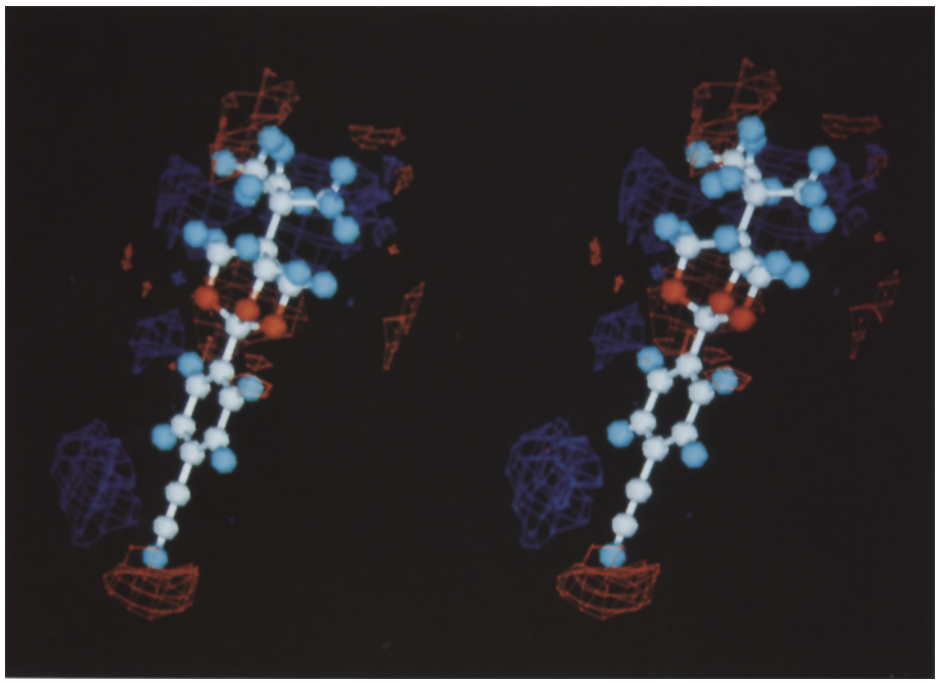

B

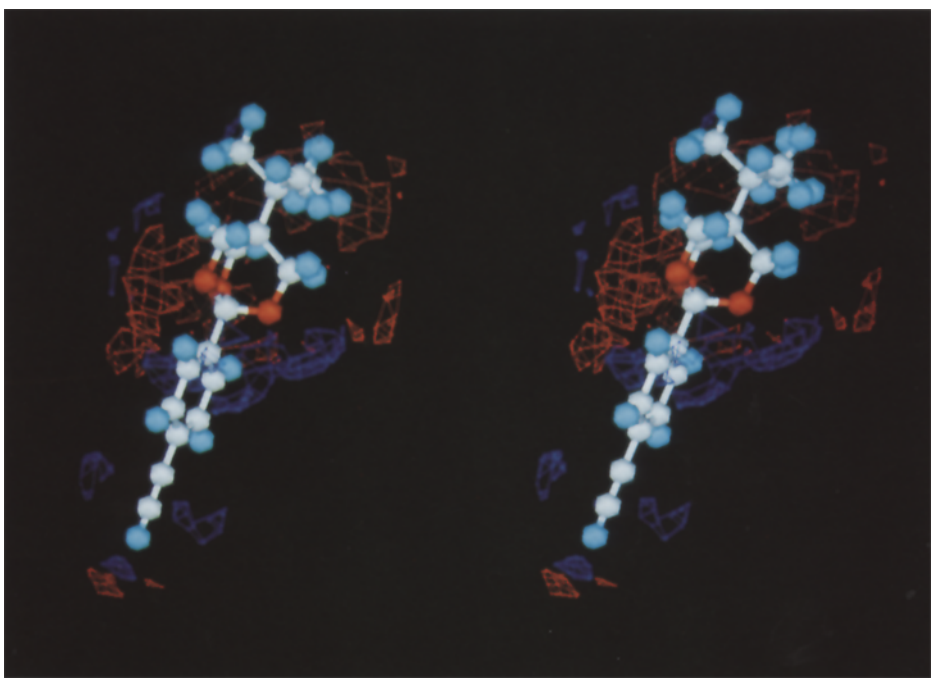

Fig. 5. (A) Steric CoAMF fields for the in vivo data; (B) Electrostatic CoMFA fields for the in vivo data.

A

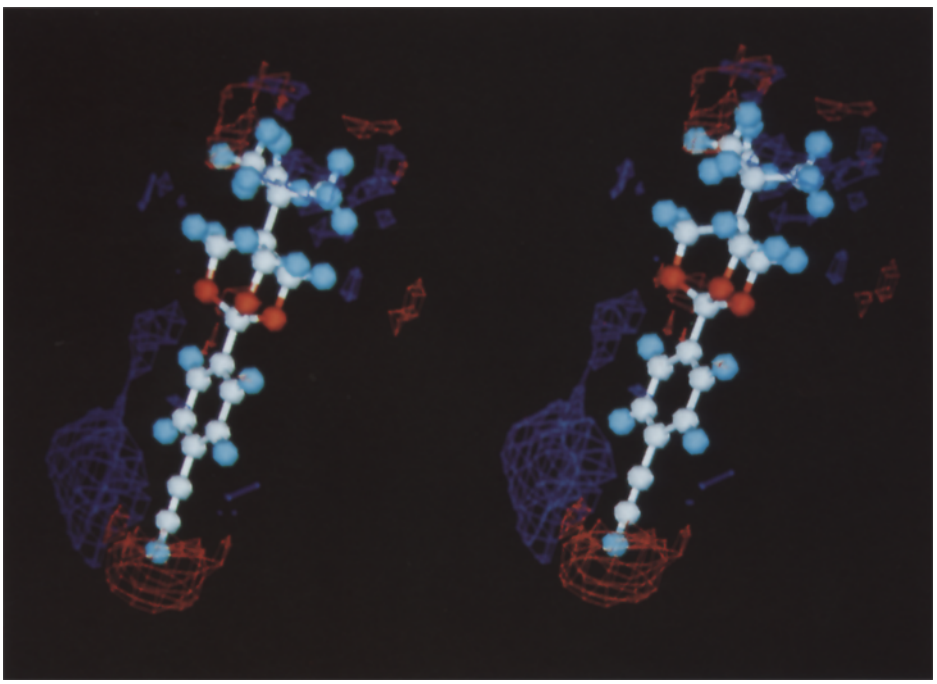

B

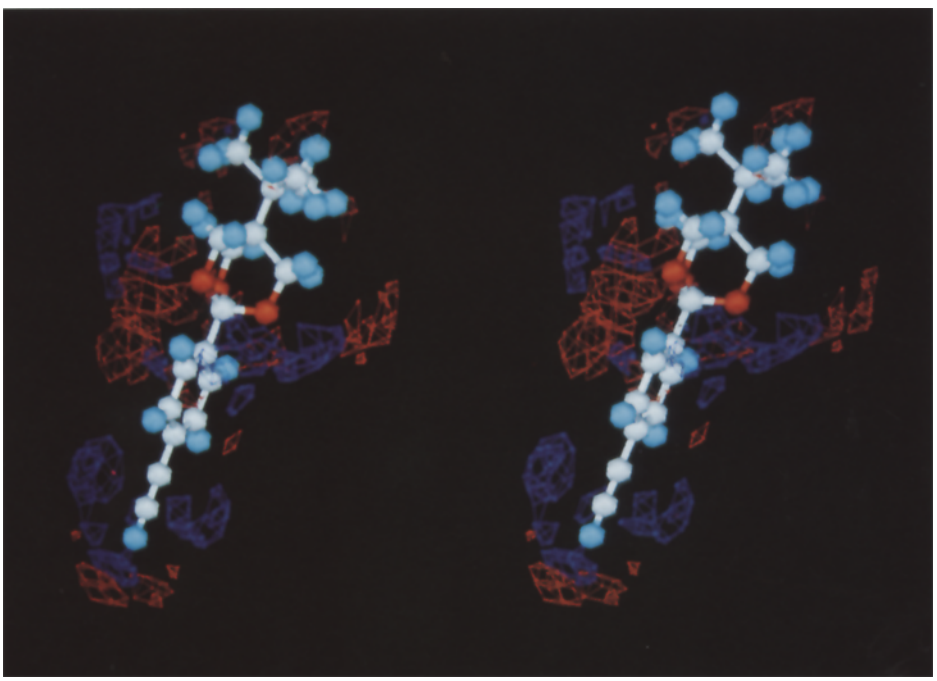

Fig. 6. (A) Steric CoAMF fields for the in vitro data; (B) Electrostatic CoMFA fields for the in vitro data.

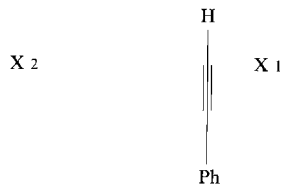

Fig. 7. Unsymmetric placement of grid points leading to poorly interpretable fields.

change in grid spacing need not affect the number of components or the quality of the model used to derive the QSAR. Attempting to interpret this asymmetric field, however, could mislead the chemist when it comes to consideration of future compounds for synthesis. Indeed, in the present example, the predictive R^2 value using a 2 Å grid spacing was only slightly smaller than that found using the 0.75 Å grid. However, in view of the desire to use CoMFA fields as an aid to structural optimisation, all subsequent runs were carried out with a 0.75 Å grid spacing.

CONCLUSION

The present study evaluated the proposal [4] that there is a common ligand binding site for a number of antagonists of the GABA-gated chloride ion channel. The steric and electrostatic alignment program was used to predict a credible overlay of six of these structurally diverse classes of insecticide (36 compounds in total). By using the orientation of these overlays relative to a common template, i.e., picrotoxinin, it was possible to derive a practical QSAR, using a CoMFA-based regression analysis. If the various chemical classes were acting at different sites, little or no correlation would have been expected between their biological activities and their steric and electrostatic fields. However, as an apparent correlation was found when using both in vivo and in vitro data, this investigation lends support to the theory that the ligand binding site for these six classes of structurally diverse insecticides is either overlapping or identical.

ACKNOWLEDGEMENTS

This study was supported in part by United States NIH grant 5 PO1 ES00049.

REFERENCES

1 Emmett, C.J. (Ed.) Comprehensive Medicinal Chemistry, Vol. 3, Pergamon Press, 1990, Oxford, pp. 493–537.
2 Vicini, S., Mienville, J. and Costa, E., J. Pharmacol. Expt. Therapeut., 243 (1987) 1195.
3 Klunk, W.E., Kalman, B.L., Ferrendelli, J.A. and Covey, D.F., Mol. Pharmacol., 23 (1983) 511.
4 Deng, Y., Palmer, J.C. and Casida, J.E., Pestic, Biochem. Physiol., 41 (1991) 60.
5 Palmer, C.J. and Casida, J.E., J. Agric. Food. Chem., 33 (1985) 976.
6 Palmer, C.J., Cole, L.M., Larkin, J.P., Smith, I.H. and Casida, J.E., J. Agric. Food. Chem., 39 (1991) 1329.
7 Cramer, R.D., Patterson, D.E. and Bunce, J.D., J. Am. Chem. Soc., 110 (1988) 5959.
8 Smith, G.A., Steric and Electrostatic Alignment Program Molecular Superposition Program, Merck Sharp & Dohme Research Laboratories, West Point, Pennsylvania 19486. Program obtained through Quantum Chemistry Program Exchange, Indiana, Bloomington (QCPE 567).
9 Stewart, J.J.P., J. Comp. Chem., 10 (1989) 209.
10 Cramer, R.D., Bunce, J.D., Patterson, D.E. and Frank, I.E., Quant. Struct.-Act. Relat., 7 (1988) 18.
11 Ozoe, Y. and Matsumura, F., J. Agric. Food. Chem., 34 (1986) 126.